Transient host-guest complexation to control catalytic activity

Michelle P. van der Helm[1], Guotai Li[1], Muhamad Hartono[1] and Rienk Eelkema*,[1]
[1] Department of Chemical Engineering, Delft University of Technology,
Van der Maasweg 9, 2629 HZ Delft, The Netherlands

***Corresponding Author:** Rienk Eelkema
Tel: +31 (0)15 27 81035; E-mail: R.Eelkema@tudelft.nl.

Keywords: Host-guest chemistry, responsive catalysis, organocatalysis, out-of-equilibrium, ester hydrolysis, chemical signals

Abstract

Signal transduction mechanisms are key to living systems. Cells respond to signals by changing catalytic activity of enzymes. This signal responsive catalysis is crucial in the regulation of (bio)chemical reaction networks (CRNs). Inspired by these networks, we report an artificial signal responsive system that shows signal-induced temporary catalyst activation. We use an unstable signal to temporarily activate an out of equilibrium CRN, generating transient host-guest complexes to control catalytic activity. Esters with favourable binding towards the cucurbit[7]uril (CB[7]) supramolecular host are used as fleeting signals to form a transient complex with CB[7], replacing a CB[7]-bound guest. The esters are hydrolytically unstable, generating acids and alcohols, which do not bind to CB[7], leading to guest re-uptake. We demonstrate the feasibility of the concept using signal-controlled temporary dye release and re-uptake. The same fleeting signal controlled system was then used to tune the reaction rate of aniline catalysed hydrazone formation. Varying the ester structure and concentration gave access to different catalyst liberation times and free catalyst concentration, regulating the overall reaction rate. With fleeting signal controlled transient complex formation we can tune the kinetics of a second chemical reaction, in which the signal does not participate. This system shows promise for building more complex non-biological networks, to ultimately arrive at signal transduction in organic materials.

Nature is full of elegant and complex signal transduction mechanisms to control key cellular processes. Cells respond to external and internal signals by altering enzymatic activity via covalent chemistry involving phosphorylation [1] or non-covalently by allosteric activation or inhibition [2-3]. Yet, artificial chemical reaction networks (CRNs) with similar complexity and control as found in living systems remain out of reach. Minimal signal integration in organic materials or reaction networks is uncommon. [4-7] Incorporation of signal responsive catalysis in such systems is key to the regulation of artificial complex CRNs, reminiscent of their natural analogues.[8] Some examples of signal-responsive catalysis have been reported for synthetic systems.[9-11] A key feature of natural signal transduction is that the change in catalytic activity is temporary, i.e. over time the catalytic activity returns to a background level. This effect is achieved by depletion of the signal, or by active deactivation of the catalyst (e.g. by dephosphorylation). In contrast, in artificial systems, catalyst turn on is most often permanent, limiting potential for application.[12-13] Here, we report a signal responsive catalyst that shows temporary catalytic activity. We achieve temporary activation with a tunable duration through the use of unstable signal molecules. Specifically, we use a combination of temporarily activated chemical reaction networks and host-guest chemistry to exert control over catalytic activity.

The last decade witnessed a steep rise in the design of chemical reaction networks that are driven away from equilibrium by the conversion of a chemical fuel. [14-16] There, a fuel molecule is used as a sacrificial reagent to drive an otherwise unfavorable chemical reaction, giving rise to non-equilibrium product distributions, transiently stable structures and unusual system behaviors (i.e. oscillations, instabilities or chaotic behavior).[14, 17-20] Non covalent interactions are frequently exploited to access transient structures, such as in the ATP-driven systems from Prins [21-24] and in the multitude of transient supramolecular polymer systems assembled from (non)-biological building blocks [17, 25-29]. At the same time, host-guest chemistry has proven a powerful tool to regulate reactivity of guest molecules, for example to control dissipative catalysis [30] or fuel-driven transient crystallization [31]. Here, in continuation of our previous work, we use cucurbit[7]uril (CB[7]) as a supramolecular host to encapsulate guest molecules in aqueous environment.[9-10] CB[7] has a high binding affinity for hydrophobic and positively charged molecules.[32] We exploit this property to temporarily push a CRN away from equilibrium via transient complex formation with an unstable signal molecule that acts analogous to a chemical fuel. Inspired by the fuel-driven systems from the Walther group[33], we use various hydrolytically unstable esters as fleeting signals to form a transient complex with CB[7]. The esters compete for CB[7] binding with the catalyst of the second chemical reaction, in this case aniline catalyzed hydrazone formation, and their hydrolysis controls the liberation of the catalyst from CB[7] and hence the catalytic activity and the overall reaction rate (Figure 1). First, we explain the design of the CRN and the choice of the fleeting signal. Next, we demonstrate the proof-of-concept by controlling dye replacement. Finally, we show precise control over the rate of the organocatalytic chemical reaction supported by a kinetic model.

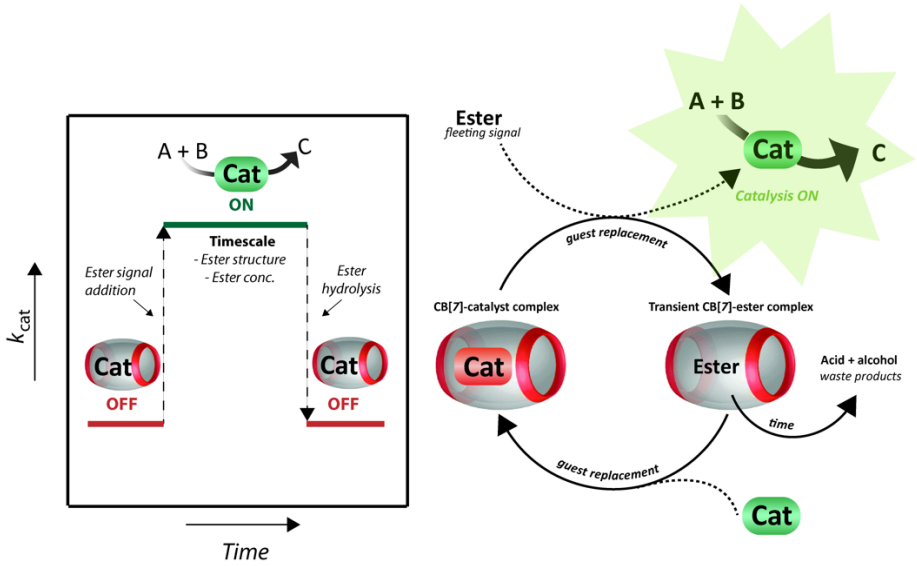

Figure 1: Transient complex formation of hydrolysable ester signals with CB[7] to control the rate of a chemical reaction by catalyst capture and release. k_{cat} (represents the catalytic rate constant) versus time is shown, responding to ester addition and ester hydrolysis (left). Cat = catalyst

For the design of this CRN, the first requirement for the ester signals is a moderate to high binding affinity with CB[7]. Secondly, they should be hydrolysable within the timescale of a catalytic chemical reaction. Thirdly, the generated carboxylic acid and alcohol should have no binding affinity towards CB[7]. Hence, we considered glycine betaine esters as the ideal candidates and three different varieties were synthesized: methyl **1**, ethyl **2** and isopropyl **3** (see SI for synthesis procedures). The positive charge from the ammonium gives favorable binding properties towards CB[7] [32], resulting in binding constants (K_a in M^{-1}) of order 10^4-10^5 (Table S1). Their binding inside CB[7] was also confirmed by NMR studies (SI Figures S3-5). Amino acid esters are activated towards hydrolysis due to the neighboring α-amino group. Additionally, the positively charged betaine increases the hydrolysis rate compared to uncharged amino acid esters. [34] Furthermore, the acid and alcohol hydrolysis products of the esters show no binding towards CB[7] (Table S1). The hydrolysis rates of the esters were measured at different pH and in the presence of CB[7] (SI Figures S6-7). Resulting from electron donating and steric effects, the hydrolysis rate displays the following order: methyl (fast) > ethyl > isopropyl (slow). Logically, a higher pH increases the ester hydrolysis rate and the presence of CB[7] slows down the hydrolysis. In the presence of CB[7] the hydrolysis of the isopropyl ester is even almost entirely switched off (SI Figure S7C,D)

We used a fluorescent dye replacement study as a proof-of-concept transient binding assessment (Figure 2). We use acridine orange (AO) **5**, which has a pK_a of 9.8 and is predominantly present in the protonated form at pH 7.5. The fluorescence intensity of the AO dye **5** is known to increase when bound inside CB[7]. [35-37] Initially, the fluorescence intensity of AO and CB[7] at 525 nm (maximum in emission spectrum) is about 0.5 (Start in Figure 2 shown as green bar).

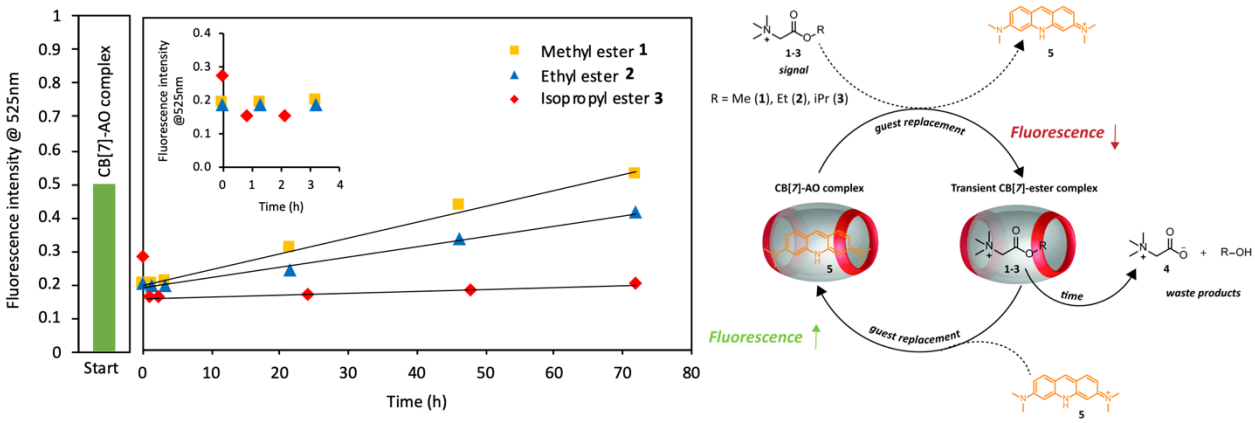

Figure 2: Fluorescence intensity of acridine orange (AO) **5** in and outside CB[7] over time at 525 nm (maximum in emission spectrum) with addition of different esters. The fluorescence intensity for **5** increases inside CB[7] (Start – green column). When the esters replace the dye inside CB[7] the fluorescence intensity decreases. The fluorescence intensity increases again when the esters hydrolyze over time and the dye is captured inside CB[7]. Conditions: esters (2.68 mM methyl **1**, 0.67 mM ethyl **2** or 0.13 mM isopropyl **3**) with 0.038 mM CB[7]and 0.027 mM AO **5** in sodium phosphate buffer 100 mM pH 7.5 at RT. Samples were excited at wavelength 465 nm.

As is apparent from Figure 2, when the esters are added the fluorescence intensity drops, which indicates that the esters replace the dye inside CB[7]. The drop in fluorescence intensity happens instantaneously for methyl **1** and ethyl ester **2**. However, for isopropyl ester **3**, where because of the higher binding constant only a low concentration is needed to reach the same percentage of transient ester⊂CB[7] complex, the initial drop is more gradual (Figure 2, S11). Over time the esters hydrolyze, generating glycine betaine **4** and an alcohol as waste products. Due to the negative charge on **4** the binding affinity for CB[7] is lost and the dye is slowly captured inside the now vacant CB[7] again. This process is demonstrated by the increase in fluorescence over time in Figure 2. In accordance to the height of the hydrolysis rate constants for the different esters (SI Figures S6-7), the fluorescence intensity increases more rapidly for methyl ester **1**, followed by ethyl ester **2** and finally isopropyl ester **3**. Thus, the chemical structure of the ester signal has a direct and strong effect on the replacement rate. Overall, with this dye replacement experiment we illustrate that we can control the rate of a second process (i.e. dye capture and release) by controlling transient complex formation through a fleeting signal.

Taking this one step further, we use the same transient complex formation strategy to control catalytic activity in time. In our previous work we showed that CB[7] can be used to control aniline **6** catalyzed hydrazone formation in a buffered system.[10] Here, we exploit the same reaction between aldehyde **7** and hydrazide **8** to form hydrazone **9** in combination with the hydrolysable esters to achieve transient control over the reaction rate (Figure 3A). In order to measure the reaction rate and determine the rate constant, the yield of hydrazone product **9** is determined with UV-Vis by following the absorbance at 287 nm (see SI Hydrazone UV-VIS absorbance and reaction kinetics). As we confirmed previously, aniline **6** binds moderately strong to CB[7] with a K_a of $2.78 \cdot 10^4$ M^{-1} and the reactants and product do not bind to CB[7] (SI Figure S1 and Table S1). To illustrate the change in reaction rate we calculated the reaction rate constant over time for the various conditions and different time intervals: with only catalyst; catalyst with CB[7] and catalyst with varying concentrations of ester signals **1-3** (Figures 3B-G and see SI Figures S13-14 for the yield of hydrazone **9** and the slopes for the determination of the rate constants). With 0.2 mM

catalyst **6** hydrazone formation is accelerated with a rate constant of 0.081 $mM^{-1}h^{-1}$, whereas by addition of 0.42 mM CB[7] a rate decrease is observed with a rate constant of 0.025 $mM^{-1}h^{-1}$. The reaction is not completely switched off due to a background reaction with constant 0.014 $mM^{-1}h^{-1}$ (SI Figure S18) and with 0.42 mM CB[7] only 87% of catalyst is complexed with CB[7], together giving the observed non-zero rate constant. Upon addition of the ester signals a guest replacement takes place. The esters replace the catalyst inside CB[7], liberating the catalyst, which in turn starts to accelerate the hydrazone formation. However, over time the esters hydrolyze and the catalyst is gradually captured inside CB[7] again. This behavior is illustrated by a decrease in the reaction rate constant (Figures 3B-G black lines). For the ester experiments we calculated the reaction rate constant for various time intervals based on the changing slopes (SI Figures S13-15). Because of small deviations in the UV data, the time intervals had to remain large (SI Figures S13-15). Especially at the end of the measurement time the deviations become larger and hence larger time intervals were used (SI Figure S15).

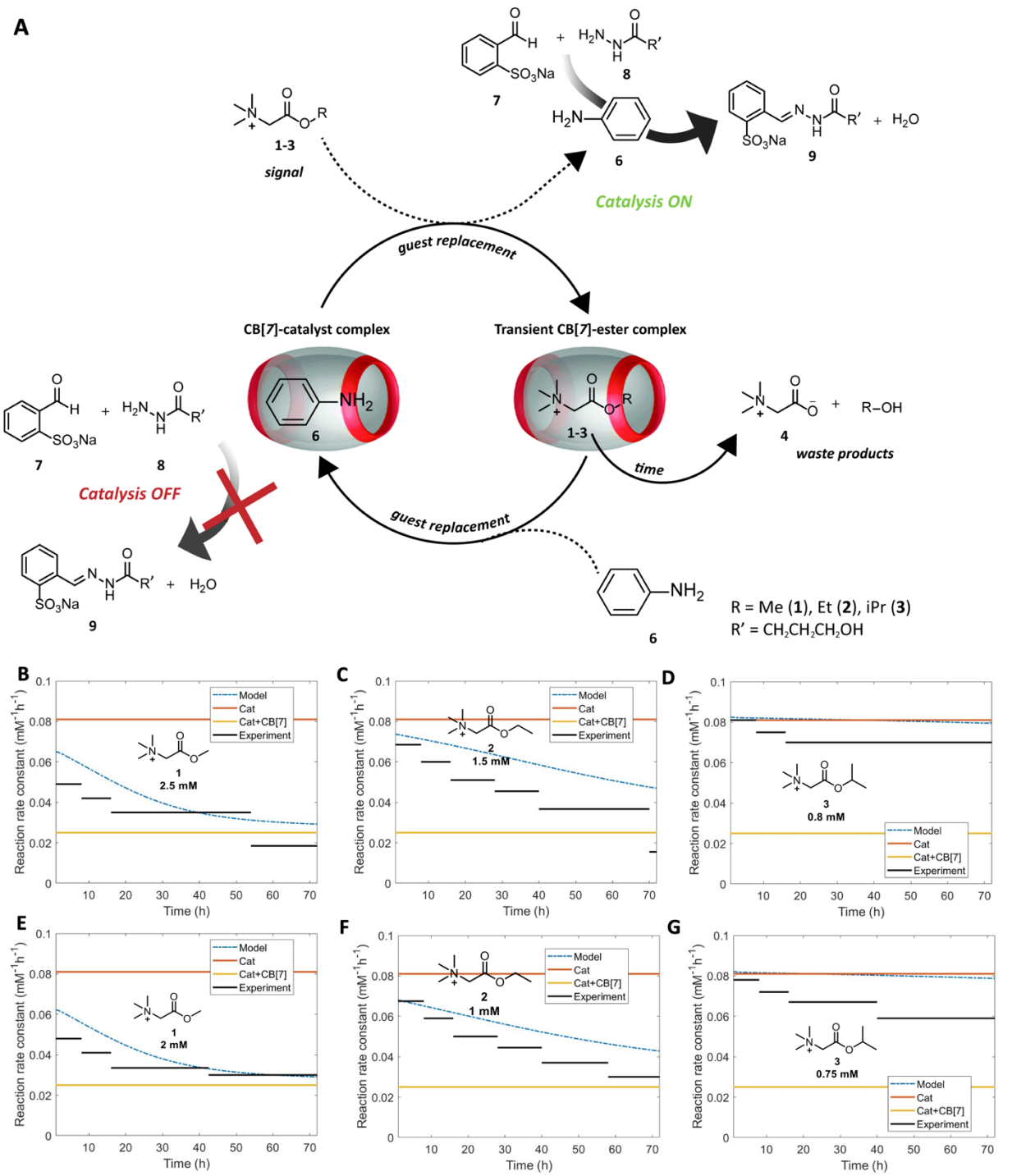

Figure 3: (A) Transient complex formation of hydrolysable ester signals with CB[7] to control the rate of hydrazone formation by aniline catalyst **6** capture and release. Rate constant for hydrazone formation as a function of time at various catalytic conditions. Values extracted from experimental data with ester signals (black lines) are compared with the model (blue dashed line): **(B)** Methyl ester **1** 2.5 mM, **(C)** Ethyl ester **2** 1.5 mM, **(D)** Isopropyl ester **3** 0.8 mM, **(E)** Methyl ester **1** 2 mM, **(F)** Ethyl ester **2** 1 mM and **(G)** Isopropyl ester **3** 0.75 mM. Conditions: pH 7.5, 100 mM phosphate buffer; 0.2 mM aldehyde **7**, 0.02 mM hydrazide **8**, 0.2 mM catalyst **6** and 0.42 mM CB[7].

Overall, the ester structure and concentration control the decrease in reaction rate and the final hydrazone **9** product yield. With 2.5 mM methyl ester **1** the catalysis is switched off after about 50 h (Figure 3B) with

61% yield of hydrazone **9** after 168 h (SI Figure S13A), whereas with [**1**]=2 mM the switch off time reduces to 40 h (Figure 3E) with 65% hydrazone **9** yield after 168 h (SI Figure S14A). For 1.5 mM ethyl ester **2** the switch off time is about 70 h (Figure 3C black line) showing 67% yield of hydrazone **9** after 168 h (SI Figure S13C) and for 1 mM of **2** about 60 h (Figure 3F black line) with 69% yield of **9** after 168 h (SI Figure S14C). However, the isopropyl ester **3** almost resembles a permanent guest, as with both 0.8 and 0.75 mM the reaction rate hardly reduces over time (Figure 3D and 3G black lines), both concentrations of **3** give 90% yield of hydrazone **9** after 168 h (SI Figure S13E, S14E). The rate constant of the reaction changes over time due to a changing free catalyst concentration in solution as a consequence of the ester hydrolysis. Using the equilibrium relations of esters and catalyst with CB[7] and the previously determined ester hydrolysis rate constants in and outside CB[7], we designed a kinetic model to determine the concentration of all the species over time (see SI Kinetic model and Figures S16-17). Based on the free catalyst concentration as a function of time we calculate the changing rate constant for hydrazone formation over time and compare it with the experimental data. As is apparent from Figures 3B-G (blue dashed lines) the modelled rate constant describes the general trend shown by the experimental data accurately for varying ester structures and concentrations. Although there are quantitative differences between the model and the measured data, the decay profile of the rate constant is described qualitatively by the model within the limits set by the catalyzed and inhibited rate constant values (horizontal lines).

Instead of adding the esters from the start, an *in-situ* catalyst activation experiment was also performed (Figure 4). At the start the rate of all experiments is similar to the catalyst⊂CB[7] experiment. Yet, when the ester signals are added after 8 h, they effectively replace the catalyst inside CB[7]. Hence, in Figure 4B-D after ester addition a rate increase is observed, indicating that catalyst **6** is liberated, accelerating the hydrazone formation. Next, upon ester hydrolysis a gradual decay in rate is observed. The decrease in rate constant and the final yield of hydrazone **9** follows a similar trend as in Figure 3 with the methyl ester **1** hydrolyzing the fastest (lowest yield of **9**) and the isopropyl ester **3** the slowest (highest yield of **9**). Also for the *in-situ* catalyst activation, the numerical model predicts the decrease in rate constant accurately but qualitatively for the different esters. For the methyl ester **1** the model rate prediction is substantially higher from the start, possibly due to some ester hydrolysis already occurring. In all, by transient complex formation with unstable ester signals inside a supramolecular host we have control over and can numerically predict the rate of a second chemical reaction by tuning the catalyst liberation time and hence the free catalyst concentration in solution.

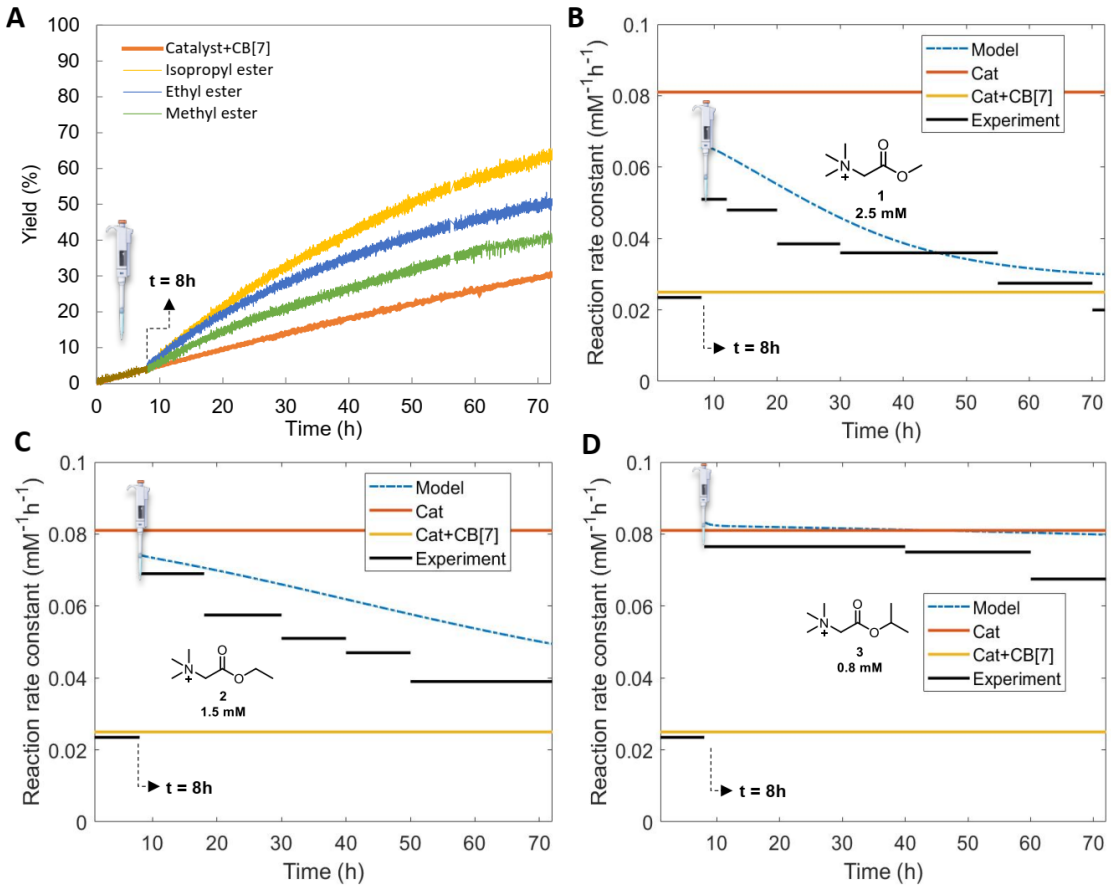

Figure 4: (A) Yield of hydrazone **9** for *in-situ* addition of esters **1-3** at t= 8h. Rate constant for hydrazone formation as a function of time at various catalytic conditions. Experimental data with ester signals (black lines) are compared with the model (blue dashed line): **(B**) Methyl ester **1** 2.5 mM, **(C)** Ethyl ester **2** 1.5 mM and **(D)** Isopropyl ester **3** 0.8 mM. Conditions: 0.2 mM aldehyde **7**, 0.02 mM hydrazide **8**, 0.2 mM catalyst **6** and 0.42 mM CB[7].

In this work, we used hydrolysable esters as fleeting signals to control catalytic activity in time. The system is based on an unstable signal molecule binding to a supramolecular host, leading to expulsion and activation of a catalyst bound in the host cavity. Decay of the signal molecule leads to reuptake and deactivation of the catalyst. As unstable signals, we used glycine betaine esters, with favourable binding towards CB[7]. Since the esters are unstable under aqueous conditions, they hydrolyse to form non-binding acids and alcohols. With the transient ester CB[7] complexes, we demonstrated temporary dye release and reuptake, showing the feasibility of the concept. Next, we increased the network complexity and introduced a second chemical reaction. We used the fleeting signal controlled transient complex formation to tune the reaction rate of aniline catalysed hydrazone formation. Altering the ester structure and concentration gave different catalyst liberation times and changed the concentration of free catalyst and the overall reaction rate. The ester signals were effectively used for *in-situ* activation of the organocatalyst. The experimental data were supported by a kinetic model. With transient complex formation we are able to control the kinetics of a second process, in which the signal itself does not take part (i.e. dye capture or chemical product formation). This generic non-equilibrium CRN, based on ester hydrolysis and supramolecular encapsulation, shows promise for building more complex non-biological networks. The non-covalent (de)activation of catalysis could be applied to signal responsive soft materials,

similar to the covalent (de)activation[13]. Altogether, this work is a first step forward towards incorporation of signal transduction in artificial materials and chemical reaction networks.

Associated content

Author information

Corresponding Author
* (R.E.) E-mail: R.Eelkema@tudelft.nl.

Notes

The authors declare no competing financial interest.

Author Contributions

M.H. and M.P.v.d.H carried out the experiments and analyzed the results. G.L. analyzed the ITC data and improved Matlab modelling. M.P.v.d.H. wrote the manuscript. M.P.v.d.H, M.H. and R.E. designed the experiments. R.E. conceived and directed the overall research project and revised the manuscript. All authors commented on the work and the manuscript.

Acknowledgement

Generous funding by the European Research Council (ERC consolidator grant 726381) is acknowledged.

References

1. G. Burnett and E. P.Kennedy, The enzymatic phosphorylation of proteins, *J. Biol. Chem.*, 1954, **211**, 969-980.
2. J. Monod, J. Changeux and F. Jacob, Allosteric Proteins and Cellular Control Systems, *J. Mol. Biol.*, 1963, **6**, 306-329.
3. A. Cornish-Bowden, Understanding allosteric and cooperative interactions in enzymes, *FEBS J.* 2014, **281**, 621–632.
4. B. S. Pilgrim, D. A. Roberts, T. G. Lohr, T. K. Ronson and J. R. Nitschke, Signal transduction in a covalent post-assembly modification cascade, *Nat. Chem.* 2017, **9**, 1276-1281.
5. P. A. Korevaar, C. N. Kaplan, A. Grinthal, R. M. Rust and J. Aizenberg, Non-equilibrium signal integration in hydrogels, *Nat. Comm.*, 2020**, 11**, 386.
6. H. Kim, M. S. Baker and S. T. Phillips, Polymeric materials that convert local fleeting signals into global macroscopic responses, *Chem. Sci.*, 2015, **6**, 3388-3392.
7. A. A. Pogodaev, A. S. Y. Wong and W. T. S. Huck, Photochemical Control over Oscillations in Chemical Reaction Networks, *J. Am. Chem. Soc.*, 2017, **139**, 15296-15299.
8. M. P. van der Helm, T. de Beun and R. Eelkema, On the use of catalysis to bias reaction pathways in out-of-equilibrium systems, *Chem. Sci.,* 2021, **12**, 4484-4493.
9. T. G. Brevé, M. Filius, C. Araman, M. P. van der Helm, P. L. Hagedoorn, C. Joo, S. I. van Kasteren and R. Eelkema, Conditional Copper-Catalyzed Azide-Alkyne Cycloaddition by Catalyst Encapsulation, *Angew. Chem. Int. Ed.,* 2020, **59**, 9340-9344.
10. G. Li, F.Trausel, M. van der Helm, B. Klemm, T. Breve, S. van Rossum, M. Hartono, H. Gerlings, M. Lovrak, J. van Esch and R. Eelkema, Tuneable control over organocatalytic activity through host guest chemistry, *Angew. Chem. Int. Ed.*, 2021, **60**, 14022-14029.
11. V. Blanco, D. A. Leigh and V. Marcos, Artificial switchable catalysts, *Chem*. *Soc. Rev.,* 2015, **44**, 5341-5370.
12. C. Maity, F.Trausel and R. Eelkema, Selective activation of organocatalysts by specific signals, *Chem. Sci.,* 2018, **9**, 5999-6005.
13. F. Trausel, C. Maity, J. M. Poolman, D. Kouwenberg, F.Versluis, J. H. van Esch and R. Eelkema, Chemical signal activation of an organocatalyst enables control over soft material formation, *Nat. Comm.* 2017, **8**, 879.
14. S. A. P. van Rossum, M. Tena-Solsona, J. H. van Esch, R. Eelkema and J. Boekhoven, Dissipative out-of-equilibrium assembly of man-made supramolecular materials, *Chem. Soc. Rev.,* 2017, **46**, 5519-5535.
15. L. S. Kariyawasam, M. M. Hossain and C. S. Hartley, The Transient Covalent Bond in Abiotic Nonequilibrium Systems, *Angew. Chem. Int. Ed.,* 2021, **60**, 12648-12658.
16. K. Das, L. Gabrielli and L. J. Prins, Chemically Fueled Self-Assembly in Biology and Chemistry, *Angew. Chem. Int. Ed*., 2021, **60**, 20120-20143.
17. J. Boekhoven, W. E. Hendriksen, G. J. M. Koper, R. Eelkema and J. H. van Esch, Transient assembly of active materials fueled by a chemical reaction, *Science,* 2015, **349**, 1075-1079.
18. J. Leira-Iglesias, A. Tassoni, T. Adachi, M. Stich and T. M. Hermans, Oscillations, travelling fronts and patterns in a supramolecular system, *Nat. Nanotechnol.*, 2018, **13**, 1021.
19. M. Tena-Solsona, B. Rieß, R. K. Grötsch, F. C. Löhrer, C. Wanzke, B. Käsdorf, A. R. Bausch, P. Müller-Buschbaum, O. Lieleg and J. Boekhoven, Non-equilibrium dissipative supramolecular materials with a tunable lifetime, *Nat. Comm.* 2017, **8**, 15895.
20. J. Boekhoven, A. M. Brizard, K. N. K. Kowlgi, G. J. M. Koper, R. Eelkema and J. H. van Esch, Dissipative Self-Assembly of a Molecular Gelator by Using a Chemical Fuel, *Angew. Chem. Int. Ed.* 2010, **122**, 4935-4938.

21. C. Pezzato and L. J. Prins, Transient signal generation in a self-assembled nanosystem fueled by ATP, *Nat. Comm.* 2015, **6**, 7790.
22. P. S. Muñana, G. Ragazzon, J. Dupont, C. Z. J. Ren, L. J. Prins and J. L. Y. Chen, Substrate‐Induced Self‐Assembly of Cooperative Catalysts, *Angew. Chem. Int. Ed.* 2018, **57**, 16469-16474.
23. S. Chandrabhas, M. Olivo, and L. J. Prins, Template-dependent (Ir)reversibility of noncovalent synthesis pathways, *ChemSystemsChem*, 2020, **2**, e1900063.
24. L. J. Prins and M. A. Cardona, ATP-fuelled self-assembly to regulate chemical reactivity in the time domain, *Chem. Sci.* 2020, **11**, 1518-1522.
25. S. Debnath, S. Roy and R. V. Ulijn, Peptide nanofibers with dynamic instability through nonequilibrium biocatalytic assembly, *J. Am. Chem. Soc.,* 2013, **135**, 16789-16792.
26. A. Sorrenti, J. Leira-Iglesias, A. Sato and T. M. Hermans, Non-equilibrium steady states in supramolecular polymerization, *Nat. Comm.*, 2017, **8**, 15899.
27. S. Dhiman, A. Jain and S. J. George, Transient helicity: fuel‐driven temporal control over conformational switching in a supramolecular polymer, *Angew. Chem. Int. Ed.*, 2017, **129**, 1349-1353.
28. D. Spitzer, L. L. Rodrigues, D. Straßburger and M. Mezger, P. Besenius, Tuneable transient thermogels mediated by a pH‐and redox‐regulated supramolecular polymerization, *Angew. Chem. Int. Ed.,* 2017, **56**, 15461-15465.
29. R. Otter, C. M. Berac, S. Seiffert and P. Besenius, Tuning the life-time of supramolecular hydrogels using ROS-responsive telechelic peptide-polymer conjugates, *Eur. Polym. J.,* 2019, **110**, 90-96.
30. C. Biagini, S. D. Fielden, D. A. Leigh, F. Schaufelberger, S. D. Stefano and D. Thomas, Dissipative Catalysis with a Molecular Machine, *Angew. Chem. Int. Ed.*, 2019, **131**, 9981-9985.
31. S. Choi, R. D. Mukhopadhyay, Y. Kim, I. C. Hwang, W. Hwang, S. K. Ghosh, K. Baek and K. Kim, Fuel‐Driven Transient Crystallization of a Cucurbit [8]uril‐Based Host-Guest Complex, *Angew. Chem. Int. Ed.* 2019, **131**, 17006-17009.
32. S. J. Barrow, S. Kasera, M. J. Rowland, J. del Barrio and O. A. Scherman, Cucurbituril-based molecular recognition, *Chem. Rev*. 2015, **115**, 12320-12406.
33. L. Heinen, T. Heuser, A. Steinschulte and A. Walther, Antagonistic enzymes in a biocatalytic pH feedback system program autonomous DNA hydrogel life cycles. *Nano Lett.* 2017, **17**, 4989-4995.
34. R. Hay, L. Porter and P. Morris, The basic hydrolysis of amino acid esters, *Aust. J. Chem.* 1966, **19**, 1197-1205.
35. M. Shaikh, J. Mohanty, P. K. Singh, W. M. Nau and H. Pal, Complexation of acridine orange by cucurbit [7]uril and β-cyclodextrin: photophysical effects and pKa shifts. *Photochem, Photobiolog. Sci.,* 2008, **7**, 408-414.
36. J. Liu; N. Jiang, J. Ma and X. Du, Insight into unusual downfield NMR shifts in the inclusion complex of acridine orange with cucurbit [7]uril. *Eur. J. Org. Chem.* 2009, **2009**, 4931-4938.
37. R. N. Dsouza, U. Pischel and W. M. Nau, Fluorescent dyes and their supramolecular host/guest complexes with macrocycles in aqueous solution, *Chem. Rev.,* 2011, **111**, 7941-7980.

Graphical abstract